

Article

Improved Model-Based Rao and Wald Test for Adaptive Range-Spread Target Detection [†]

Haoxuan Xu [‡], Jiabao Liu [‡] and Meiguo Gao ^{* }

School of Information and Electronics, Beijing Institute of Technology, Beijing 100081, China; haoxuan_xu1999@163.com (H.X.); liujiabao747@163.com (J.L.)

* Correspondence: meiguo_g@bit.edu.cn

[†] This paper is an extended version of our paper published in ICET: Liu, J.; Xu, H.; Chen, Z.; Gao, M. Improved Model-Based Rao and Wald Test for Adaptive Range-Spread Target Detection. In Proceedings of the 2021 IEEE 4th International Conference on Electronics Technology (ICET), Chengdu, China, 7–10 May 2021; pp. 1223–1228. <https://doi.org/10.1109/ICET51757.2021.9450915>.

[‡] Co-first author—these authors contributed equally to this work.

Abstract: This article addresses the problem of the detection of range-spread targets in the presence of Gaussian disturbance which are in possession of unidentified covariance matrices. The detectors have been derived by resorting to a design composed of two steps. Based on the Rao test and Wald test, the corresponding strategies of detection were respectively derived, assuming the expression of disturbance covariance matrix has been obtained. Afterwards, the unknown parameters in the detectors were estimated on the basis of both the primary and the training data, utilizing the autoregressive property of the disturbance. A remarkable characteristic of the Rao and Wald detectors is they both asymptotically attain constant false-alarm rate (CFAR) in respect of the disturbance covariance matrix. Finally, we completed a performance assessment by utilizing the simulated data, and the result demonstrated the effectiveness of the existing proposals compared with the detectors previously proposed.

Keywords: Rao test; Wald test; autoregressive; range-spread target



Citation: Xu, H.; Liu, J.; Gao, M. Improved Model-Based Rao and Wald Test for Adaptive Range-Spread Target Detection. *Electronics* **2022**, *11*, 1248. <https://doi.org/10.3390/electronics11081248>

Academic Editors: Chua-Chin Wang and Arezki Benfdila

Received: 3 May 2021

Accepted: 16 March 2022

Published: 15 April 2022

Publisher's Note: MDPI stays neutral with regard to jurisdictional claims in published maps and institutional affiliations.



Copyright: © 2022 by the authors. Licensee MDPI, Basel, Switzerland. This article is an open access article distributed under the terms and conditions of the Creative Commons Attribution (CC BY) license (<https://creativecommons.org/licenses/by/4.0/>).

1. Introduction

Over the past few decades, there has been more and more attention in the field of detecting range-spread targets adaptively in the presence of disturbance which is described by unknown covariance matrix [1–3]. The point-like target model is invalid with the extensively application of the high resolution radars (HRRs), which have the ability to resolve a target into multiple scattering centers appearing into different range cells [4]. Based on relevant theories of the generalized likelihood ratio test (GLRT), adaptive detectors have been developed specially for range-spread targets in recent last decades [2,5], which estimate all the unidentified parameters separately under each hypothesis. Moreover, the design of the detectors have absorbed relevant theories of the Rao and Wald tests, which not only perform with less complexity and stronger robustness than the GLRT, but also have the same asymptotic performance as the latter [6]. Specifically, by applying theories of the Rao test and Wald test, related scholars have successfully proposed constant false-alarm rate (CFAR) detectors in the case of homogeneous scenarios [7], where the disturbance covariance matrices of range cells under test are entirely identical to those of training data. In [8,9], the disturbance respectively described as a spherically invariant random process (SIRP) as well as complex Gaussian distribution are taken into consideration. In [10], the problem of adaptively detecting multichannel signal in homogeneous Gaussian disturbance and the generalization of the generalized multivariate analysis of variance (GMANOVA) are thoroughly researched. Additionally, similar works of adaptive detection of subspace signals are also considered [11,12].

For the achievement of the detection performance within 3 dB of the optimal threshold, it is required to set the training data number to no less than two times the data dimension according to [13]. However, this condition could not always be met in several practical applications, especially in heterogeneous scenarios [14] and dense-target [15] scenarios. Fortunately, exploiting the autoregressive (AR) property of the disturbance can effectively reduce the data set required for the estimation of unknown parameters [16]. Specifically, Kay proposed an AR-based generalized likelihood ratio (ARGLR) detector for the circumstance of a target known up to a scaling factor by way of exploiting AR process in his GLRT detector. Moreover, to effectively detect range-spread targets, a growing number of AR-based detectors have been derived resorting to the adaptive matched filter (AMF) [17], the Rao test [18] and so on. However, these detectors would suffer severe performance degradation when the data record is relatively small since M (the order of the AR process) samples are discarded [19].

Motivated by the works mentioned above and based on our previous relevant work [20], we derived adaptive detectors for range-spread targets without discarding samples by reconstructing the covariance matrix based on the AR parameters [21] specifically for the small data problem. More concretely, to respectively derive the detection strategies in the scenario of Rao test and Wald test is the first step. After this, the covariance matrices of the disturbance are constructed using the maximum likelihood estimation of AR coefficients under each hypothesis. Eventually, the conclusion can be summed up by analyzing simulation results, which demonstrates that the proposed improved autoregressive-Rao (IAR-Rao) and improved autoregressive-Wald (IAR-Wald) detectors have the ability to achieve a higher level of detection performance than existing ones for small data record. The remainder of the paper is organized as follows. Section 2 introduces the process of problem formulation, while the method and detailed design of the Rao and Wald detectors is explained in Section 3. Section 4 provides the performance assessments of newly proposed detectors. Finally, Section 5 gives a conclusion of our study. From the conclusion, it is indicated that the proposed IAR-Rao and IAR-Wald detectors are able to achieve a detection performance improvement compared to the regular AR-Rao and AR-Wald, especially in the limited training case, while both the newly derived detectors are asymptotically CFAR, which means the detection performance of both approaches that of the optimum matched filter for large data record case. Additionally, both the detectors are proved to be effective based on the analysis of real data.

The symbols and notations which are frequently used in this article are stated as:

- H_0 : The hypothesis which there exists no target;
- H_1 : The hypothesis which there exist a target;
- \mathbf{z}_t : The collected complex data vector;
- α_t : The unknown amplitude of corresponding scatterer of the target.;
- \mathbf{n}_t : The disturbance vector;
- \mathbf{p} : The steering vector;
- $[\cdot]^T$: The transpose operation of the matrix;
- $[\cdot]^\dagger$: The conjugate transpose operation of the matrix;
- $E\{\cdot\}$: The statistical expectation operator;
- \mathbf{M} : The covariance matrix of the disturbance vector;
- \mathbf{L} : The lower triangular matrix after applying factorization to the covariance matrix;
- \mathbf{D} : The real diagonal matrix after applying factorization to the covariance matrix.

2. Problem Formulation

Our research is based on a radar system which collects data using a coherent N -pulse train, as well as detecting the presence of a range-spread target across L range cells. Moreover, there exists an available set of training data, which is collected through sampling from K range cells. When it comes to the t -th range cell individually, the corresponding

procedure of detection will obey the rule of the binary hypothesis test which has the following form:

$$\begin{cases} H_0 : z_t = \mathbf{n}_t & t = 1, \dots, L + K \\ H_1 : z_t = \alpha_t \mathbf{p} + \mathbf{n}_t & t = 1, \dots, L + K \end{cases} \quad (1)$$

Here, $z_t \in C^N$ (C stands for the vector of complex data) represents the data vector in N -dimensional space collected from the t -th range cell ($t = 1, 2, \dots, L + K$), and is respectively referred to as primary data ($t = 1, \dots, L$) and secondary data ($t = L + 1, \dots, L + K$), while the latter may also be referred to as the training data. α_t describes the unknown amplitude corresponding to the scatterer of the target in the t -th range cell ($t = 1, \dots, L$), which simultaneously takes the channel effects as well as the target reflectivity into consideration. The steering vector has an expression of $\mathbf{p} = [\mathbf{1}, e^{j\Omega}, \dots, e^{j(N-1)\Omega}]^T$, here Ω is the target Doppler which is assumed to be perfectly known and $[\cdot]^T$ denotes transpose operation. The disturbance vectors, which are expressed by \mathbf{n}_t , are modelled as independent and identically distributed (IID) zero mean complex Gaussian vectors of which the covariance matrix is identical.

$$E\{\mathbf{n}_t \mathbf{n}_t^\dagger\} = \mathbf{M} \quad (2)$$

where the statistical expectation operator is expressed by $E\{\cdot\}$, \dagger denotes conjugate transpose operation.

By using the theory of Therrien [21], the AR coefficients and the noise power of \mathbf{n}_t are related to the covariance matrix through the following factorization

$$\mathbf{M} = \mathbf{L} \mathbf{D} \mathbf{L}^\dagger \quad (3)$$

In the formula above, \mathbf{L} indicates a lower triangular matrix and the rows of its inversion are the coefficients of the AR process of \mathbf{n}_t from orders 0 to $N - 1$. \mathbf{D} stands for a real diagonal matrix and its elements are the corresponding white noise power of \mathbf{n}_t .

3. Detectors Design

Aiming to examine detection problem in (1), we have adopted the two-step Rao and Wald test procedures as described in [7], respectively. On the basis of Rao test and Wald test, it is firstly required to derive the detection strategies respectively and correspondingly under the assumption of known disturbance covariance matrix \mathbf{M} . Afterwards, by using the primary and the training data, an estimation value of \mathbf{M} is plugged into the test statistic by way of utilizing the AR property of the disturbance, which makes both of the algorithms adaptive.

3.1. Detectors Design with Known \mathbf{M}

With the aim of deriving the test statistics of the Rao test and the Wald test, a denotation is proposed as $\boldsymbol{\theta} = [\alpha_{1,R}, \alpha_{1,I}, \alpha_{2,R}, \alpha_{2,I}, \dots, \alpha_{L,R}, \alpha_{L,I}]^T$, which stands for a real column vector with $2L$ dimensions, the real part as well as the imaginary part of α_t are expressed by $\alpha_{t,R}$ and $\alpha_{t,I}$ ($t = 1, \dots, L$).

3.1.1. Rao Test with Known \mathbf{M}

In the previously mentioned situation at hand, the Rao test obeys the decision rule described as followed [22].

$$\frac{\partial \ln f(z_1, \dots, z_{L+K} | \boldsymbol{\theta}, \mathbf{M})}{\partial \boldsymbol{\theta}} \Big|_{\boldsymbol{\theta}=\hat{\boldsymbol{\theta}}_0}^T \left[\mathbf{J}^{-1}(\hat{\boldsymbol{\theta}}_0) \right] \times \frac{\partial \ln f(z_1, \dots, z_{L+K} | \boldsymbol{\theta}, \mathbf{M})}{\partial \boldsymbol{\theta}} \Big|_{\boldsymbol{\theta}=\hat{\boldsymbol{\theta}}_0} \underset{H_0}{\overset{H_1}{\geq}} \eta_r \quad (4)$$

Here we have

- η_r is defined as the threshold of detection which is set with the purpose of ensuring the desired probability of false alarm (P_{fa});
- $\partial/\partial\theta = [\partial/\partial\alpha_{1,R}, \partial/\partial\alpha_{1,I}, \dots, \partial/\partial\alpha_{L,R}, \partial/\partial\alpha_{L,I}]^T$;
- J represents the Fisher information matrix (FIM);
- $\hat{\theta}_0$ is used to describe the maximum likelihood estimate (MLE) of θ under hypothesis H_0 ;
- $f(z_1, \dots, z_{L+K} | \theta, M)$ is the denotation used to describe the probability density function (PDF) of the data under hypothesis H_0 , which can be expressed as

$$f(z_1, \dots, z_{L+K} | \theta, M) = \frac{1}{\pi^{N(L+K)} \|\mathbf{M}\|^{L+K}} \times \exp \left\{ - \left[\sum_{t=1}^L (z_t - \alpha_t \mathbf{p})^\dagger \mathbf{M}^{-1} (z_t - \alpha_t \mathbf{p}) + \sum_{t=L+1}^{L+K} z_t^\dagger \mathbf{M}^{-1} z_t \right] \right\} \quad (5)$$

For the problem at hand, the results are easily computed as

$$\frac{\partial f}{\partial \alpha_{t,R}} = 2 \operatorname{Re} \left\{ \mathbf{p}^\dagger \mathbf{M}^{-1} (z_t - \alpha_t \mathbf{p}) \right\} \quad (6)$$

$$\frac{\partial f}{\partial \alpha_{t,I}} = 2 \operatorname{Im} \left\{ \mathbf{p}^\dagger \mathbf{M}^{-1} (z_t - \alpha_t \mathbf{p}) \right\} \quad (7)$$

$$[J^{-1}(\theta)] = \frac{1}{2} (\mathbf{p} \mathbf{M}^{-1} \mathbf{p})^{-1} \mathbf{I}_{2L \times 2L} \quad (8)$$

and

$$\hat{\theta}_0 = \mathbf{0}_{2L \times 1} \quad (9)$$

where $\mathbf{I}_{2L \times 2L}$ indicates the $2L \times 2L$ -dimensional identity matrix, $\mathbf{0}_{2L \times 1}$ is the $2L$ -dimensional zero vector.

Substituting (6)–(9) into (4) followed by some algebra, the following formula can be used to describe the Rao test

$$\frac{\sum_{t=1}^L \left| \mathbf{p}^\dagger \mathbf{M}^{-1} z_t \right|_{H_1}^2}{\mathbf{p}^\dagger \mathbf{M}^{-1} \mathbf{p}} \underset{H_0}{\overset{H_1}{\geq}} \eta_r \quad (10)$$

3.1.2. Wald Test with Known M

The following decision rule can thoroughly represent the Wald test [23]

$$(\hat{\theta}_1 - \theta_0)^T [J^{-1}(\hat{\theta}_1)]^{-1} (\hat{\theta}_1 - \theta_0) \underset{H_0}{\overset{H_1}{\geq}} \eta_w \quad (11)$$

where

- η_w represents the detection threshold which is set to ensure the desired P_{fa} ;
- $\hat{\theta}_1 = [\hat{\alpha}_{1,R}, \hat{\alpha}_{1,I}, \dots, \hat{\alpha}_{L,R}, \hat{\alpha}_{L,I}]^T$ is an expression applied to indicate the MLE of θ under hypothesis H_1 .

Through the utilization of the structure of the FIM according to (8), we can rewrite the Wald test as

$$\hat{\theta}_1^T J(\hat{\theta}_1) \hat{\theta}_1 \underset{H_0}{\overset{H_1}{\geq}} \eta_w \quad (12)$$

Moreover

$$\hat{\alpha}_t = \frac{\mathbf{p}^\dagger \mathbf{M}^{-1} z_t}{\mathbf{p}^\dagger \mathbf{M}^{-1} \mathbf{p}} \quad (13)$$

Hence, substituting (8) and (13) into the decision rule (12) followed by some algebraic operations, it is possible to obtain the Wald test with known M

$$\frac{\sum_{t=1}^L \left| \mathbf{p}^\dagger \mathbf{M}^{-1} \mathbf{z}_t \right|^2}{\mathbf{p}^\dagger \mathbf{M}^{-1} \mathbf{p}} \underset{H_0}{\overset{H_1}{\gtrless}} \eta_w \tag{14}$$

According to (10) and (14), the detectors are accomplished once M is acquired. For the estimation of M , it is efficient to adopt several methods on the basis of the sufficient training data (see, e.g., [24,25]). Unfortunately, when it comes to realistic scenarios, this requirement cannot be satisfied all the time. Thus, for the purpose of achieving better detection performance under limited-training cases, we resort to the theory of Therrien [21] and utilize the AR property of the disturbance to reconstruct M . The relevant information is to be shown in the next subsection.

3.2. Estimation of M Based on AR Parameters

As mentioned in [18], the disturbance is described as a an AR process model of order P , coefficient \mathbf{a} , and noise power σ^2 . In the Rao test, all of these parameters can be obtained by calculating their MLEs respectively under hypothesis H_0 , while the operations are conducted under hypothesis H_1 for the Wald test. Once the MLEs are obtained, the covariance matrices M_0 and M_1 can be reconstructed according to (3). Precisely, $\hat{M}_0 = L_0 D_0 L_0^\dagger$ and $\hat{M}_1 = L_1 D_1 L_1^\dagger$, where

$$L_0^{-1} = \begin{bmatrix} 1 & 0 & 0 & \cdots & 0 \\ -\hat{\mathbf{a}}_0(1) & 1 & 0 & \cdots & 0 \\ -\hat{\mathbf{a}}_0(2) & -\hat{\mathbf{a}}_0(1) & 1 & \cdots & 0 \\ \vdots & \vdots & \ddots & \vdots & \vdots \\ 0 & 0 & \cdots & -\hat{\mathbf{a}}_0(1) & 1 \end{bmatrix} \tag{15}$$

$$D_0 = \hat{\sigma}_0^2 \mathbf{I}_{N \times N} \tag{16}$$

$$L_1^{-1} = \begin{bmatrix} 1 & 0 & 0 & \cdots & 0 \\ -\hat{\mathbf{a}}_1(1) & 1 & 0 & \cdots & 0 \\ -\hat{\mathbf{a}}_1(2) & -\hat{\mathbf{a}}_1(1) & 1 & \cdots & 0 \\ \vdots & \vdots & \ddots & \vdots & \vdots \\ 0 & 0 & \cdots & -\hat{\mathbf{a}}_1(1) & 1 \end{bmatrix} \tag{17}$$

$$D_1 = \hat{\sigma}_1^2 \mathbf{I}_{N \times N} \tag{18}$$

Here, $\hat{\mathbf{a}}_0$ and $\hat{\sigma}_0^2$ are obtained by maximizing the joint PDF given in [15] with respect to \mathbf{a} and σ^2 respectively under hypothesis H_0 . The results are given as:

$$\hat{\mathbf{a}}_0 = - \left(\sum_{t=1}^{L+K} \mathbf{X}_t^\dagger \mathbf{X}_t \right)^{-1} \left(\sum_{t=1}^{L+K} \mathbf{X}_t^\dagger \mathbf{u}_t \right) \tag{19}$$

$$\hat{\sigma}_0^2 = \frac{\mathbf{1}}{(N-P)(L+K)} \left[\sum_{t=1}^{L+K} (\mathbf{u}_t + \mathbf{X}_t \hat{\mathbf{a}}_0)^\dagger (\mathbf{u}_t + \mathbf{X}_t \hat{\mathbf{a}}_0) \right] \tag{20}$$

where \mathbf{X}_t and \mathbf{u}_t are defined in [23]. When it comes to $\hat{\mathbf{a}}_1$ and $\hat{\sigma}_1^2$, there is a projection matrix which is defined as $\mathbf{H} = \mathbf{I} - \frac{\boldsymbol{\varphi} \boldsymbol{\varphi}^\dagger}{\boldsymbol{\varphi}^\dagger \boldsymbol{\varphi}}$, here we have:

$$\boldsymbol{\varphi} = \left[1, \dots, e^{j(N-P-1)\Omega} \right]^\text{T} \tag{21}$$

$$\hat{a}_1 = - \left(\sum_{t=1}^L X_t^\dagger H X_t + \sum_{t=L+1}^{L+K} X_t^\dagger X_t \right)^{-1} \left(\sum_{t=1}^L X_t^\dagger H u_t + \sum_{t=L+1}^{L+K} X_t^\dagger u_t \right) \tag{22}$$

$$\hat{\sigma}_1^2 = \frac{1}{(N - P)(L + K)} \left[\sum_{t=1}^L (u_t + X_t \hat{a}_1)^\dagger H (u_t + X_t \hat{a}_1) + \sum_{t=L+1}^{L+K} (u_t + X_t \hat{a}_1)^\dagger (u_t + X_t \hat{a}_1) \right] \tag{23}$$

By substituting \hat{M}_0 and \hat{M}_1 into (10) and (14) respectively, we obtain the so-named improved AR-Rao detector (IAR-Rao detector) and improved AR-Wald detector (IAR-Wald detector). For the scenario of a large number of data (i.e., $N \rightarrow \infty$), both of the newly derived IAR-Rao and IAR-Wald are able to achieve the same asymptotic performance as GLRT. This prominently demonstrates that the proposed detectors are asymptotically CFAR in respect of the disturbance covariance matrix [18]. Correspondingly, Figure 1 displays a block diagram of the detectors design.

As it can be observed, Figure 1 illustrates the main concept and process of the aforementioned assumptions and derivations. Conclusively, it is firstly assumed that the covariance matrix of the disturbance is previously known, then the intermediate form of the Rao test and the Wald test is respectively derived. Afterwards, both the primary data and the secondary data are exploited to attain the autoregressive property of the disturbance. The estimation values are directly substitute to the intermediate form of the detectors and relevant decisions are evident to obtain.

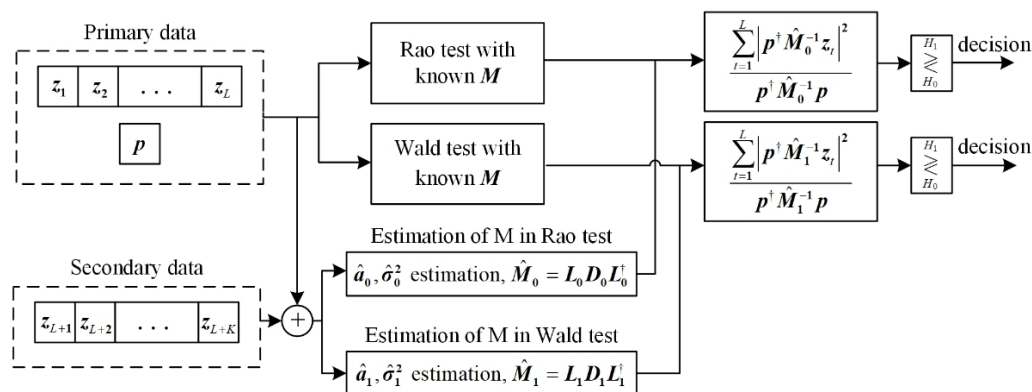


Figure 1. Block diagram of the detectors design procedure.

4. Numerical Results

In Section 4, an analysis of the detection performance of the newly derived IAR-Rao and IAR-Wald detectors is completed by utilizing the simulated data of range-spread targets. With the purpose of comparison, the tradition AR-Rao [18] and AR-Wald [26] are also taken into consideration. The definition of signal-to-noise plus interference ratio (SINR) is given by the following formula.

$$\text{SINR} = \sum_{t=1}^L |\alpha_t|^2 p^\dagger M p / L \tag{24}$$

For complex numbers, the modulus is denoted by $|\cdot|$. The disturbance signals n_t are generated with given parameters from an AR process of order 2. We apply 10^5 independent Monte Carlo trials for the purpose of estimating the thresholds, and 10^4 independent trials in order to figure out the detection probability (P_d). Moreover, we set $P_{fa} = 10^{-4}$, $\Omega = 0$ and $P = 2$.

The P_d versus SINR of the newly derived IAR-Rao and IAR-Wald are plotted in Figure 2 comparing with AR-Rao and AR-Wald. Additionally, the detection probability curve of the ideal matched filter (MF) is also drawn in Figure 2. Although the MF cannot be achieved in a realistic scenario, it provides a baseline comparison. It is quite evident that the IAR-Rao outperforms AR-Rao and IAR-Wald outperforms AR-Wald especially at high SINR. That is because the traditional methods of AR detectors discard samples of which the number is equivalent to the autoregressive order P . When the pulse number N becomes larger, the traditional AR detectors become very close to the IAR detectors. This phenomenon is caused by the truth that the number of the discarded pluses (P) can be ignored as N increases. For all of AR and the IAR detectors, there are always a performance loss compared with the MF, which can be explained as the estimated covariance matrices (\hat{M}_0 and \hat{M}_0) are always inaccurate when compared with its true value (M).

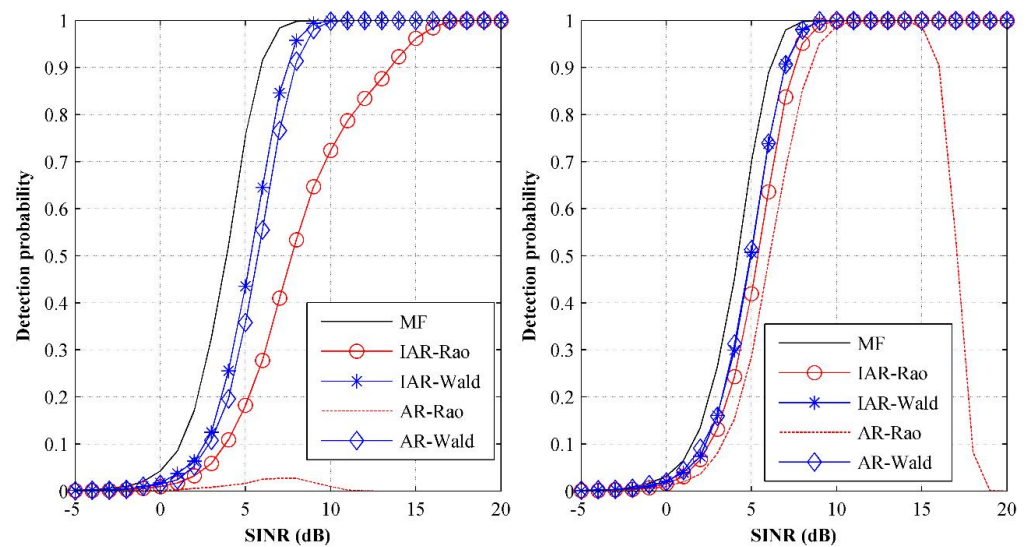


Figure 2. P_d versus SINR of the MF, of the IAR-Rao, of the IAR-Wald, of the AR-Rao, and of the AR-Wald for $L = 8$, $K = 3$ and various N . (**left**) Detection performances while setting $N = 8$; (**right**) detection performances while setting $N = 16$.

In Figure 3, we abbreviate “IAR-Rao” as “IAR-R” and “IAR-Wald” as “IAR-W”. It can be seen that the IAR-Wald detector can still achieve good detection performance under the circumstance of insufficient data for training, which is in agreement with that of AR-Rao detector. Figure 3 directly shows the AR-Rao detector performance decreases under high SNR. This is because Rao test uses both the primary and the training data to estimate the covariance matrix of the clutter. When the SINR is large, the signal is to influence and contaminate the estimated value of the clutter covariance matrix. The mentioned phenomenon does not exist in the newly derived IAR-Rao algorithm.

Figure 4 provides a display of the receiver operating characteristic (ROC) of the newly derived detectors, which is depicted respectively for various numbers of target scatterers L , while we keep $K = 0$ and $\text{SINR} = 5$ dB. By the comprehensive observation of the figure, it is clear to conclude that the performance of the proposed detection methods will grow when the L value increases. To put it differently, the detectors’ performance is capable of being improved by increasing the radar resolution. Obviously, the IAR-Wald outperforms IAR-Rao in the realistic detection environment (low P_{fa}); However, it has a heavy computation compared to the latter.

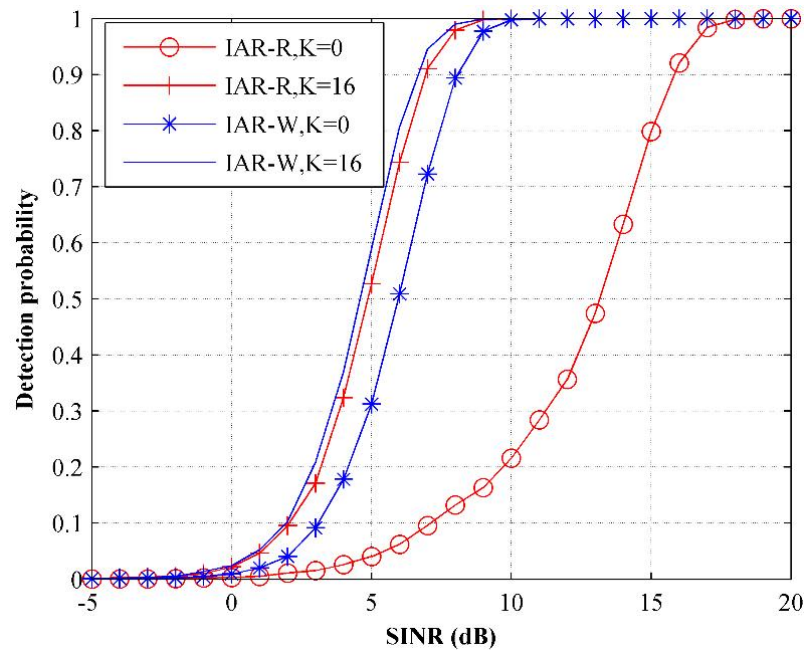


Figure 3. P_d versus SINR of the IAR-Rao and of the IAR-Wald for $N = 16$, $L = 8$, and various K .

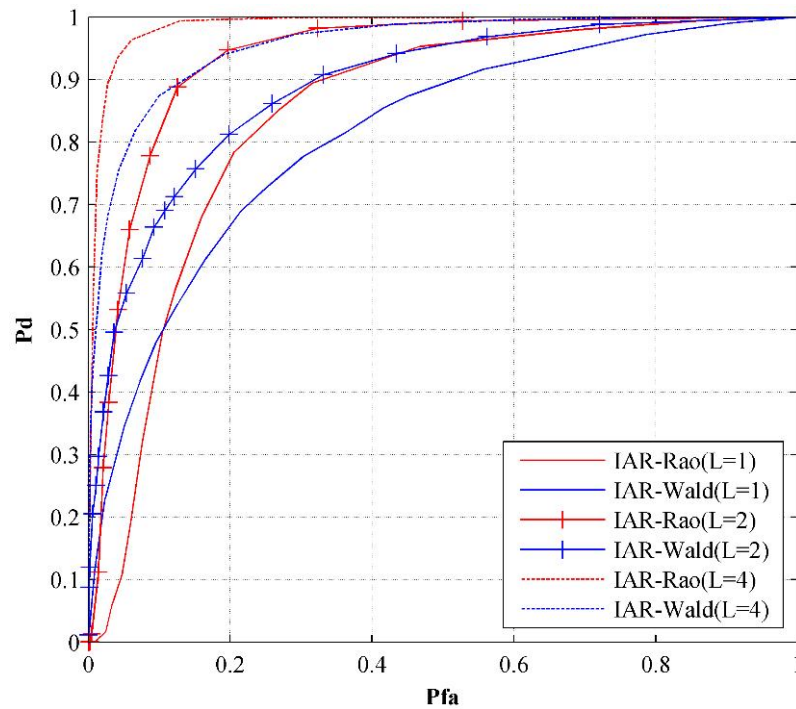


Figure 4. ROC of the IAR-Rao and of the IAR-Wald under conditions of $N = 16$, $K = 0$, SINR = 5 dB and various L .

In Figure 5 (left), we have plotted the detection curves of the conventional AR-Rao detector and the newly derived IAR-Rao detector. It can be seen that the collapse loss exists under high SINR is vanished by the method of two-step detector design. All the curves in Figure 5 indicate that both AR-Rao and AR-Wald achieve improved detection performance by means of matrix reconstruction. Moreover, the detection performance deteriorates with the increase of M for each detector, which is so-called order mismatched.

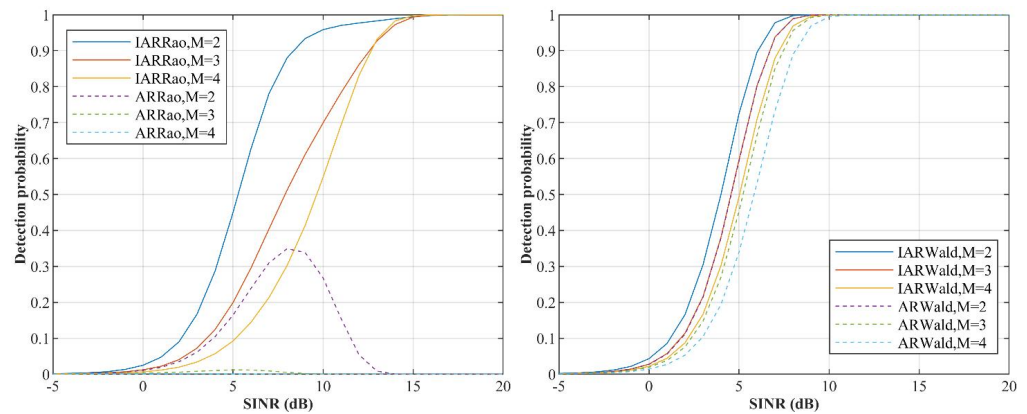


Figure 5. P_d versus SINR for $P_{fa} = 10^{-4}$, $N = 16$, $L = 8$ and $K = 3$. (left) Performances of AR-Rao and IAR-Rao; (right) performances of AR-Wald and IAR-Wald.

5. Real Data Analysis

For evaluating the performance of the two new detectors, we complete a further assessment using the high-resolution range profiles (HRRPs) gathered from the actual data of Tiangong-1, which are collected from the measurement of inverse synthesis aperture radar (ISAR). Figure 6 (left) gives a display of the original echo data, which demonstrates that range migration would occur in moving targets scenarios. Firstly, envelope alignment and self-focusing are needed to eliminate the influence of target translation. Then the IAR-Rao detector and the IAR-Wald detector are used to detect the processed data. Figure 6b shows the aligned echo. Additionally, we set $L = 80$ as the target occupies 67 range cells.

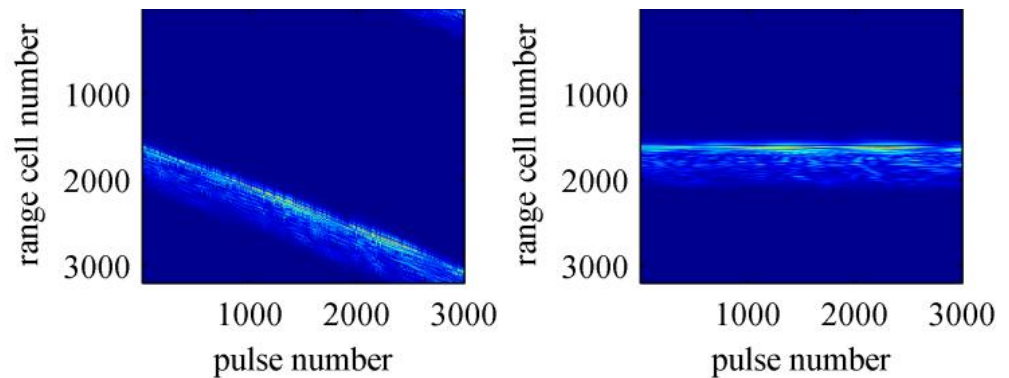


Figure 6. HRRP of Tiangong-1 collected from the measurement of inverse synthesis aperture radar. (left) Original HRRP of Tiangong-1; (right) aligned HRRP of Tiangong-1.

In order to evaluate the impact of sample number N to the performances of two detection methods, we draw corresponding detection curves in Figure 7 under the circumstance that $L = 80$ and $K = 0$. From the figure we can easily sum up that the performance of the IAR-Rao detector does not decrease at high SINR (existing in AR-Rao detector), which indicates that the performance of the newly raised and developed IAR-Rao detector is better than that of AR-Rao detector at high SINR. The four measured data curves are also close to the simulation results. Figure 8 displays the receiver operating characteristic (ROC) curves in correspondence with each detector, all of these mentioned curves are depicted under the circumstance of different L values, while keeping $K = 0$ and $SINR = -3$ dB unchanged. We are able to conclude that the detector performance improves in respect of the increase of target range number L . That is to say, it is possible to improve the detection performance by increasing the radar resolution, which is consistent with our traditional cognition.

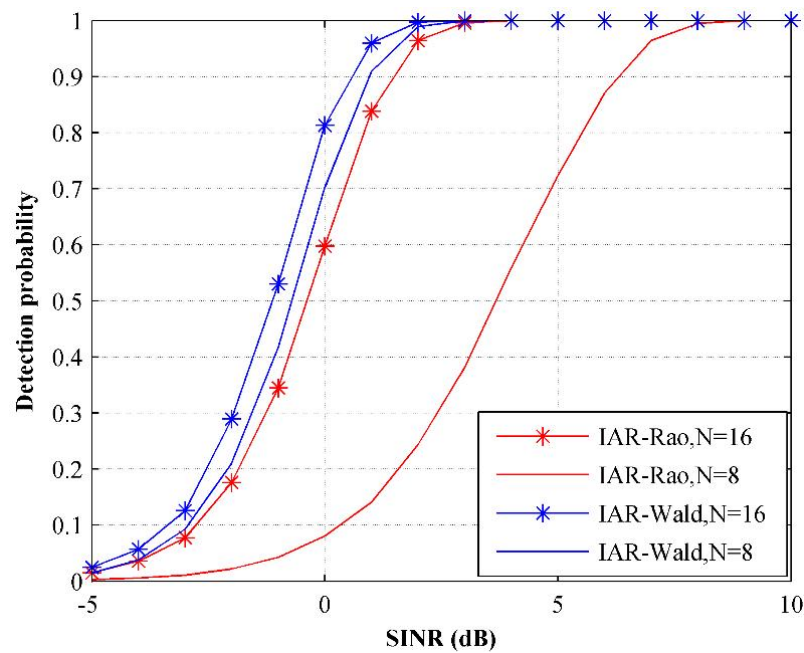


Figure 7. P_d versus SINR for $P_{fa} = 10^{-4}$, $L = 80$, $K = 0$ and various N .

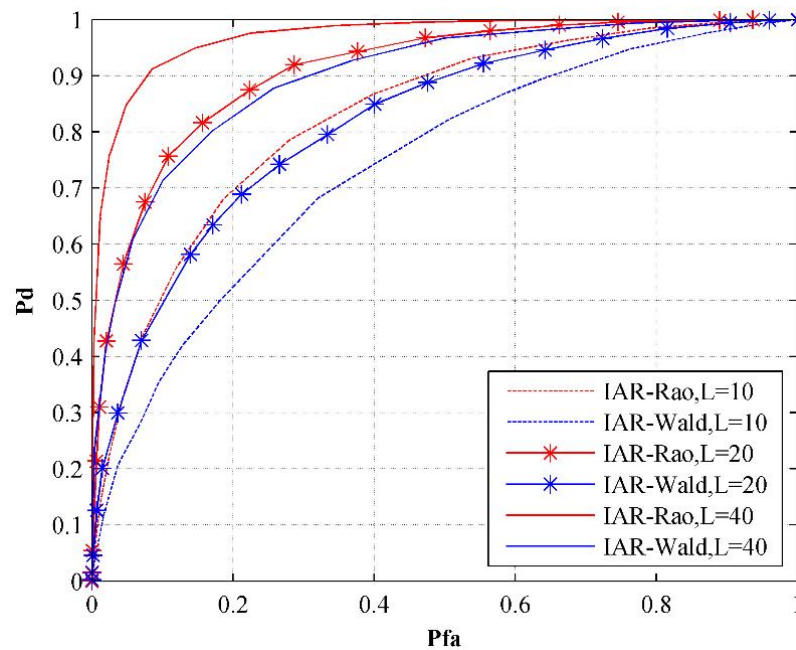


Figure 8. ROC of the AR-Wald detector for $N = 16$, $K = 0$, $SINR = -3$ dB and various L .

Results of further analysis shows the consistence of the detection results of real data and simulation data, both of which prove the effectiveness of the proposed IAR-Rao and IAR-Wald detection algorithms.

6. Conclusions

The contribution and conclusion of our study are described as follows. We successfully proposed the design of two detectors for circumstances of range-spread target detection, in the presence of disturbance which is in possession of unknown covariance, based on two-step design. An autoregressive process is used to model the disturbance, of which parameters are estimated respectively. Unlike traditional AR-based detector designs, discarding P samples, we constructed the covariance matrix based on the estimated AR

parameters resorting to the theory of the relationship between the AR process and triangular matrix decomposition. Simulation results indicate that the proposed IAR-Rao and IAR-Wald detectors achieve detection performance improvement over the regular AR-Rao and AR-Wald, especially in limited training case. Moreover, both of the newly derived detectors are asymptotically CFAR, which means the detection performance of both approached that of the optimum matched filter for large data-record cases. Both the IAR-Rao and the IAR-Wald are proved to be effective on the basis of the analysis of the real data. In the future, we will aim to utilize the two-step method based on the AR covariance estimation in order to improve the performance of the existing detectors [10,27].

Author Contributions: Conceptualization, J.L.; methodology, H.X., M.G. and J.L.; software, H.X., M.G. and J.L.; validation, M.G. and H.X.; writing—original draft preparation, J.L.; writing—review and editing, M.G. and H.X.; supervision, M.G. and H.X.; All authors have read and agreed to the published version of the manuscript.

Funding: This research received no external funding.

Conflicts of Interest: The authors declare no conflict of interest.

References

1. Gerlach, K.; Steiner, M.; Lin, F. Detection of a spatially distributed target in white noise. *IEEE Signal Process. Lett.* **1997**, *4*, 198–200. [[CrossRef](#)]
2. Conte, E.; De Maio, A.; Ricci, G. GLRT-based adaptive detection algorithms for range-spread targets. *IEEE Trans. Signal Process.* **2001**, *49*, 1336–1348. [[CrossRef](#)]
3. Jian, T.; He, Y.; Su, F.; Qu, C.; Ping, D. Adaptive detection of sparsely distributed target in non-Gaussian clutter. *IET Radar Sonar Navig.* **2011**, *5*, 780–787. [[CrossRef](#)]
4. Boers, Y.; Driessen, H.; Torstensson, J.; Trieb, M.; Karlsson, R.; Gustafsson, F. Track-before-detect algorithm for tracking extended targets. *IEE Proc.-Radar Sonar Navig.* **2006**, *153*, 345–351. [[CrossRef](#)]
5. Casillo, M.; De Maio, A.; Iommelli, S.; Landi, L. A persymmetric GLRT for adaptive detection in partially-homogeneous environment. *IEEE Signal Process. Lett.* **2007**, *14*, 1016–1019. [[CrossRef](#)]
6. Kay, S.M. *Fundamentals of Statistical Signal Processing*; Prentice Hall PTR: Hoboken, NJ, USA, 1993.
7. Conte, E.; De Maio, A. Distributed target detection in compound-Gaussian noise with Rao and Wald tests. *IEEE Trans. Aerosp. Electron. Syst.* **2003**, *39*, 568–582. [[CrossRef](#)]
8. Guan, J.; Zhang, X. Subspace detection for range and Doppler distributed targets with Rao and Wald tests. *Signal Process.* **2011**, *91*, 51–60. [[CrossRef](#)]
9. Liu, W.; Liu, J.; Huang, L.; Zou, D.; Wang, Y. Rao tests for distributed target detection in interference and noise. *Signal Process.* **2015**, *117*, 333–342. [[CrossRef](#)]
10. Ciunozzo, D.; De Maio, A.; Orlando, D. A unifying framework for adaptive radar detection in homogeneous plus structured interference—Part I: On the maximal invariant statistic. *IEEE Trans. Signal Process.* **2016**, *64*, 2894–2906. [[CrossRef](#)]
11. De Maio, A.; Orlando, D. Adaptive radar detection of a subspace signal embedded in subspace structured plus Gaussian interference via invariance. *IEEE Trans. Signal Process.* **2015**, *64*, 2156–2167. [[CrossRef](#)]
12. Ciunozzo, D.; De Maio, A.; Orlando, D. On the statistical invariance for adaptive radar detection in partially homogeneous disturbance plus structured interference. *IEEE Trans. Signal Process.* **2016**, *65*, 1222–1234. [[CrossRef](#)]
13. Reed, I.S.; Mallett, J.D.; Brennan, L.E. Rapid convergence rate in adaptive arrays. *IEEE Trans. Aerosp. Electron. Syst.* **1974**, *AES-10*, 853–863. [[CrossRef](#)]
14. Melvin, W.L. Space-time adaptive radar performance in heterogeneous clutter. *IEEE Trans. Aerosp. Electron. Syst.* **2000**, *36*, 621–633. [[CrossRef](#)]
15. Melvin, W.L.; Guerci, J.R. Adaptive detection in dense target environments. In Proceedings of the 2001 IEEE Radar Conference (Cat. No. 01CH37200), Atlanta, GA, USA, 3 May 2001; pp. 187–192.
16. Kay, S. Asymptotically optimal detection in unknown colored noise via autoregressive modeling. *IEEE Trans. Acoust. Speech Signal Process.* **1983**, *31*, 927–940. [[CrossRef](#)]
17. Wang, P.; Li, H.; Kavala, T.R.; Himed, B. Generalised parametric Rao test for multi-channel adaptive detection of range-spread targets. *IET Signal Process.* **2012**, *6*, 404–412. [[CrossRef](#)]
18. Wang, Z.; Li, M.; Lu, Y.; Zuo, L.; Zhang, P.; Wu, Y. Model-based Rao test for adaptive range-spread target detection. *Digit. Signal Process.* **2017**, *69*, 300–308. [[CrossRef](#)]
19. Shuai, X.F.; Kong, L.J.; Yang, J.Y. Improved AR-based GLRT detector for range-spread targets in compound-Gaussian clutter without secondary data. *J. Electron. Sci. Technol.* **2010**, *9*, 180–184.

20. Liu, J.; Xu, H.; Chen, Z.; Gao, M. Improved Model-Based Rao and Wald Test for Adaptive Range-Spread Target Detection. In Proceedings of the 2021 IEEE 4th International Conference on Electronics Technology (ICET), Chengdu, China, 7–10 May 2021; pp. 1223–1228.
21. Therrien, C. On the relation between triangular matrix decomposition and linear prediction. *Proc. IEEE* **1983**, *71*, 1459–1460. [[CrossRef](#)]
22. De Maio, A. Rao test for adaptive detection in Gaussian interference with unknown covariance matrix. *IEEE Trans. Signal Process.* **2007**, *55*, 3577–3584. [[CrossRef](#)]
23. De Maio, A. A new derivation of the adaptive matched filter. *IEEE Signal Process. Lett.* **2004**, *11*, 792–793. [[CrossRef](#)]
24. Van Trees, H.L. *Detection, Estimation, and Modulation Theory, Part I: Detection, Estimation, and Linear Modulation Theory*; John Wiley & Sons: Hoboken, NJ, USA, 2004.
25. Gini, F.; Greco, M. Covariance matrix estimation for CFAR detection in correlated heavy tailed clutter. *Signal Process.* **2002**, *82*, 1847–1859. [[CrossRef](#)]
26. Kejriwal, M.; Perron, P.; Zhou, J. Wald tests for detecting multiple structural changes in persistence. *Econom. Theory* **2013**, *29*, 289–323. [[CrossRef](#)]
27. Ciuonzo, D.; De Maio, A.; Orlando, D. A unifying framework for adaptive radar detection in homogeneous plus structured interference—Part II: Detectors design. *IEEE Trans. Signal Process.* **2016**, *64*, 2907–2919. [[CrossRef](#)]